Adv. Geosci., 39, 107–114, 2014
www.adv-geosci.net/39/107/2014/
doi:10.5194/adgeo-39-107-2014

Advances in Geosciences
Open Access

Particle tracking modeling of sediment-laden jets

S. N. Chan[1] **and J. H. W. Lee**[2]

[1]Croucher Laboratory of Environmental Hydraulics, The University of Hong Kong, Hong Kong. Presently: School of Civil and Environmental Engineering, Nanyang Technological University, Singapore
[2]Department of Civil and Environmental Engineering, Hong Kong University of Science and Technology, Hong Kong

Correspondence to: S. N. Chan (treechan@graduate.hku.hk)

Received: 15 October 2013 – Revised: 7 April 2014 – Accepted: 22 April 2014 – Published: 27 June 2014

Abstract. This paper presents a general model to predict the particulate transport and deposition from a sediment-laden horizontal momentum jet. A three-dimensional (3-D) stochastic particle tracking model is developed based on the governing equation of particle motion. The turbulent velocity fluctuations are modelled by a Lagrangian velocity autocorrelation function that captures the trapping of sediment particles in turbulent eddies, which result in the reduction of settling velocity. Using classical solutions of mean jet velocity, and turbulent fluctuation and dissipation rate profiles derived from computational fluid dynamics calculations of a pure jet, the equation of motion is solved numerically to track the particle movement in the jet flow field. The 3-D particle tracking model predictions of sediment deposition and concentration profiles are in excellent agreement with measured data. The computationally demanding Basset history force is shown to be negligible in the prediction of bottom deposition profiles.

1 Introduction

The transport of sediment or particulate matters in horizontal turbulent jets is common in natural and engineered environment. A river discharges as a surface horizontal buoyant jet when the ambient forcings in the receiving waterbody are small compared to the strength of outflow (Wright, 1977). The flow is characterized by a Gaussian horizontal velocity profile that spreads and decays downstream because of shearing and lateral turbulent mixing at the jet margins. Edmonds and Slingerland (2007) demonstrates that this velocity field results in a river mouth bar which controls subsequent sedimentation and delta formation patterns. Solid-containing wastewater are often discharged into coastal waters in the form of submarine horizontal buoyant jets (Fischer et al., 1979). Particulates may settle close to the source, giving rise to the formation of sludge banks, for which its impact on the benthic environment has not been well-understood.

A number of studies concerning horizontal sediment-laden (buoyant) jets have been carried out (e.g., Bleninger et al., 2002; Lane-Serff and Moran, 2005; Cuthbertson and Davies, 2008; Lee et al., 2013). Chan (2013) found that there is a significant settling velocity reduction up to 25–35 % under the influence of jet turbulence, depending on the intensity of turbulence and particle properties. For the first time, Chan et al. (2014) developed a three-dimensional (3-D) stochastic particle tracking model for predicting sediment concentration and bottom deposition and validated it with extensive experimental data of horizontal jets laden with sand and glass particles. In previous river jet studies, the importance of settling velocity modification by turbulence has not been addressed, despite a number of research carried out on explaining the morphological changes related to river jet systems (e.g., Wright, 1977; Edmonds and Slingerland, 2007; Mariotti et al., 2013).

This paper presents the development of a general stochastic particle tracking model to predict the particulate transport and the resultant bottom deposition of a horizontal particle-laden jet discharge (Fig. 1) with validation using experimental data. The present study focuses on a sediment-laden round jet in a stagnant ambient, neglecting the effects of buoyancy, and surface and bottom boundaries as in a typical river jet (Wright, 1977). Despite these substantial simplifications, the study aims to provide insight for the physics of turbulence-sediment interaction through experimental and numerical modeling investigations. It also address the importance of Basset force in governing the particle motion and deposition in turbulent jet flows, which has not been studied previously with experimental data.

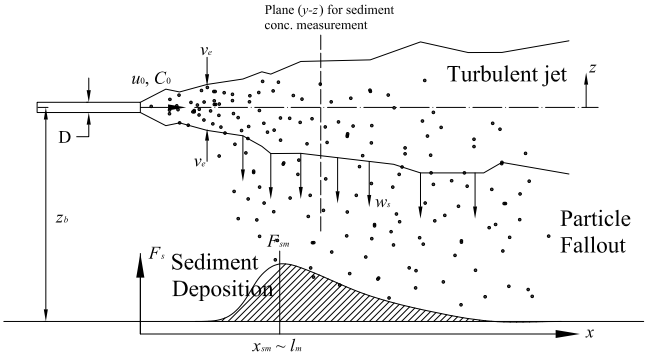

Figure 1. A horizontal sediment-laden round jet and its longitudinal bottom deposition (transversely lumped) profile.

2 Problem Definition

Figure 1 shows a schematization of a horizontal sediment-laden momentum round jet with dilute concentration. The jet with diameter D and initial average velocity across the jet orifice u_0 mixes with ambient fluid by shear induced turbulent entrainment. As observed in the present and previous experiments (Bleninger et al., 2002; Lee et al., 2013), sediment (concentration C_0 and settling velocity w_s) are transported in the horizontal direction and dispersed by turbulent mixing. Particles gradually fall out from the jet, forming a bottom deposition profile with a peak near the jet nozzle and an elongated tail.

The behaviour of a dilute sediment-laden jet is characterized by u_0, D, C_0 and w_s respectively. The sediment deposition rate per unit distance along jet direction F_s ($\mathrm{g\,m^{-1}\,s^{-1}}$) has a peak value at the distance x_{sm}. Bleninger et al. (2002) and Lee et al. (2013) proposed that when the radial entrainment velocity v_e (proportional to the local characteristic jet velocity) is less than the settling velocity w_s, particles start to fall out from the jet. Thus a momentum-settling length scale $l_m = M_0^{1/2}/w_s$ ($M_0 = u_0^2 \pi D^2/4$ = jet initial momentum) can be devised, which is a measure of the distance from the source to the location where sediment starts to fall out from the jet. It represents the importance of jet momentum-induced velocity relative to settling velocity (Cuthbertson and Davies, 2008; Lee et al., 2013).

3 Numerical particle tracking model

3.1 Governing equation of particle motion

The Lagrangian particle tracking approach is used to model a particle-laden jet. The idea is to predict the motion of a large number of particles ($N_p = 50\,000$) released from the jet nozzle, based on the equation of motion of a spherical particle in an unsteady, non-uniform fluid flow field:

$$\begin{aligned}\rho_p V_p \frac{d\mathbf{u}_p}{dt} &= (\rho_f - \rho_p) V_p \mathbf{g} \\ &- \frac{1}{2}\rho_f C_D A_p \left|\mathbf{u}_p - \mathbf{u}_f\right| \left(\mathbf{u}_p - \mathbf{u}_f\right) \\ &+ \rho_f V_p \left(\frac{d\mathbf{u}_f}{dt}\right)_f \\ &- \rho_f C_M V_p \left[\frac{d\mathbf{u}_p}{dt} - \left(\frac{d\mathbf{u}_f}{dt}\right)_f\right] \\ &- \frac{3}{2} d^2 \sqrt{\pi \nu} \int_0^t \frac{\frac{d(\mathbf{u}_p - \mathbf{u}_f)}{d\tau}}{\sqrt{t-\tau}} d\tau,\end{aligned} \quad (1)$$

where $\mathbf{u}_p = (u_p, v_p, w_p)$ is the particle velocity; $\mathbf{u}_f = (u_f, v_f, w_f)$ is the fluid velocity; $V_p = \pi d^3/6$ is the volume of the particle; $A_p = \pi d^2/4$ is the projected area of the particle; ρ_p is particle density (depends on particles used); ρ_f is water density $\approx 1\,\mathrm{g\,cm^{-3}}$; $\mathbf{g} = (0, 0, -g)$ is gravitational acceleration ($g = 9.81\,\mathrm{m\,s^{-2}}$); C_D is drag coefficient taken as a function of the particle Reynolds number $Re_p = \frac{|\mathbf{u}_p - \mathbf{u}_f| d}{\nu}$, using the empirical equation of Clift et al. (1978):

$$C_D = \frac{24}{Re_p}\left(1 + 0.15 Re_p^{0.687}\right) + \frac{0.42}{1 + 42\,500\, Re_p^{-1.16}}. \quad (2)$$

$C_M = 0.5$ is the added-mass coefficient (Lamb, 1932); d is particle diameter; $\nu = \mu/\rho_f$ is fluid kinematic viscosity $\approx 10^{-6}\,\mathrm{m^2\,s^{-1}}$; and μ is dynamic viscosity $\approx 10^{-3}\,\mathrm{kg\,m^{-1}\,s^{-1}}$. t is the time from the start of computation and τ is a dummy time variable for Basset force integration.

The left hand side of Eq. (1) denotes the acceleration of the sphere and the right hand side represents the forces acting on the spherical particle: body (gravity/buoyancy), drag, fluid acceleration, added mass and Basset. The fluid velocity $\mathbf{u}_f$ is composed of the the mean flow velocity $\overline{\mathbf{u}_f}$ and the turbulent fluctuation $\mathbf{u}'_f$, which are determined based on the analytical mean flow velocity of a pure jet (Sect. 3.3) and a stochastic approach (Sect. 3.4) respectively. The particle velocity $\mathbf{u}_p$ is solved by numerical integration with the particle position $\mathbf{x}_p$ equation:

$$\mathbf{u}_p = \frac{d\mathbf{x}_p}{dt}, \quad (3)$$

using a second order predictor-corrector scheme. The particle position provides the jet mean flow velocity and the turbulent properties.

3.2 Basset force term

The Basset history force represents the temporally changing viscous shear force acting on the particle as there exists a velocity gradient between the moving particle and the ambient. The Basset term poses two challenges to the solution of the equation of particle motion (Eq. 1). Firstly, the Basset

integral has to be evaluated every time step. As t increases, the numerical integration becomes increasingly cumbersome and time-consuming with additional storage for the relative accelerations. Secondly, the integrand is ill-behaved as $\tau \to t$ and becomes a infinity.

The Basset integral (excluding the coefficient $\frac{3}{2}d^2\sqrt{\pi\nu}$) has to be evaluated by the following approach. First, the integral is decomposed into a sum of M integrals with each integrated within a small time step Δt in which $t = M\Delta t$. Secondly, relative velocity derivative $d\mathbf{u}_\mathrm{r}/dt$ is evaluated with central difference and assumed constant within the small time step Δt, thus can be separated out from the integral.

$$\int_0^t \frac{\frac{d\mathbf{u}_\mathrm{r}}{d\tau}}{\sqrt{t-\tau}} d\tau = \sum_{k=1}^{M} \left[\frac{\Delta \mathbf{u}_\mathrm{r}}{\Delta t}\right]_k \int_{(k-1)\Delta t}^{k\Delta t} \frac{d\tau}{\sqrt{t-\tau}}, \tag{4}$$

where $\mathbf{u}_\mathrm{r} = \mathbf{u}_\mathrm{p} - \mathbf{u}_\mathrm{f}$ is the particle relative velocity. The integral involving the square root is evaluated analytically as

$$\int_{(k-1)\Delta t}^{k\Delta t} \frac{d\tau}{\sqrt{t-\tau}} = 2\sqrt{\Delta t}\left(\sqrt{M-k+1} - \sqrt{M-k}\right). \tag{5}$$

The Basset integral can be evaluated as a sum of the definite integrals in Eq. (5) multiplied by the relative velocity derivative. Detailed computation implementation of the Basset force term can be found in Chan (2013).

3.3 Jet mean velocity field (analytical solution)

The extensively validated theoretical mean flow velocity field of a simple round jet is used to evaluate $\overline{\mathbf{u}_\mathrm{f}} = (u, v_r)$. The jet mean longitudinal velocities are given by (see e.g., Fischer et al., 1979)

$$\frac{u_\mathrm{c}(x)}{u_0} = 6.2\left(\frac{x}{D}\right)^{-1} \tag{6}$$

$$\frac{u(x,r)}{u_\mathrm{c}(x)} = \exp\left(-\frac{r^2}{b^2}\right), \tag{7}$$

where u_c is the jet centerline velocity, $b = \beta x$ is the Gaussian half width and $\beta = 0.114$ is the jet linear spreading rate. The mean transverse radial velocity v_r of the jet is given by (Lee and Chu, 2003)

$$\frac{v_r(r)}{\alpha u_\mathrm{c}} = \frac{\left(1-\exp(-\frac{r^2}{b^2})\right) - (\frac{\beta}{\alpha})(\frac{r^2}{b^2})\exp(-\frac{r^2}{b^2})}{r/b}, \tag{8}$$

where $v_\mathrm{e} = \alpha u_\mathrm{c}$ is the entrainment velocity at $r = b$; $\alpha = 0.057$ is the entrainment coefficient. River jets are usually described by plane jet solution due to the large width to depth ratio (e.g., Rowland et al., 2007). In a plane jet, the longitudinal jet velocity decays more slowly with distance with a power law of -0.5 (vs. -1 power law of a round jet, Eq. 6). Nevertheless, the linear spreading, the self-similar Gaussian profile of transverse velocity distribution, and the shear nature of turbulence generation are similar.

3.4 Stochastic modeling of particle turbulent fulctuations

The key to modeling settling particles in turbulence lies in the modeling of the turbulent fluctuation $\mathbf{u}'$. Nielsen (1992) postulated the "loitering" effect for which particles are trapped in turbulent eddies and delayed from settling. Nielsen (1992) developed an autocorrelation function that described this effect, assuming particles always travels with a constant downward relative velocity which equals to the stillwater settling velocity w_s. This is not always true due to finite particle inertia. We modified it to account for the varying particle velocity using the instantaneous particle velocity fluctuation (subtracted the mean flow):

$$R_i = \exp\left[-\frac{\Delta t}{T_\mathrm{E}}\sqrt{1 + A_\mathrm{E}^2\left(\frac{||\mathbf{u}_{\mathrm{p},i} - \overline{\mathbf{u}_{f,i}}||^2}{\sigma^2}\right)}\right] \tag{9}$$

where

$$||\mathbf{u}_{\mathrm{p},i} - \overline{\mathbf{u}_{f,i}}||^2 = (u_{\mathrm{p},i} - \overline{u_{f,i}})^2 + (v_{\mathrm{p},i} - \overline{v_{f,i}})^2 + (w_{\mathrm{p},i} - \overline{w_{f,i}})^2$$

In the expression, σ is the root-mean-square (RMS) velocity fluctuation. The subscript i denotes the values in the current time step. L_E and T_E are the Eulerian spatial and time scale of the turbulence respectively estimated as:

$$L_\mathrm{E} = C_\mu^{3/4}\frac{k^{3/2}}{\epsilon} \tag{10}$$

$$T_\mathrm{E} = \sqrt{\frac{3}{2}}C_\mu^{3/4}\frac{k}{\epsilon} \tag{11}$$

from the $k-\epsilon$ turbulence closure model (Launder and Spalding, 1974), where k is turbulent kinetic energy; ϵ is turbulent dissipation rate; and $C_\mu = 0.09$. σ is related to turbulent kinetic energy by $\sigma = \sqrt{\frac{2}{3}k}$. $A_\mathrm{E} = \sigma T_\mathrm{E}/L_\mathrm{E} = 1$.

It is of interest to note that R_i decreases with increasing $||\mathbf{u}_{\mathrm{p},i} - \overline{\mathbf{u}_{f,i}}||$, which means a particle with higher instantaneous velocity decorrelates faster with its previous velocity, as the argument of the exponential function becomes more negative. This results in a condition that particles stay in the upward moving flow longer than in the downward moving flow, mimicking the trapping effect and reduction of net settling velocity. Extensive numerical experiments of particle settling in homogeneous turbulence have confirmed the characteristic feature of Eq. (9) (Chan, 2013). With support from Particle Imaging Velocimetry (PIV) measurements of the jet velocity field, the generation of particle loitering effect by jet turbulence is demonstrated (Chan et al., 2014). The trapping of sediment by large coherent eddies in river jets has also been observed in a recent numerical study by Mariotti et al. (2013).

For turbulent round jet flow, assuming isotropic turbulence, σ and ϵ can be obtained from computational fluid dynamics (CFD) simulation of a pure jet using the realizable

$k-\epsilon$ turbulence closure model (Shih et al., 1995). The predicted σ and ϵ are normalized with the mean jet properties as $\frac{\sigma}{u_c}$ and $\frac{(\epsilon b)^{1/3}}{u_c}$ respectively, and fitted with an equation with the form of

$$\frac{\sigma}{u_c} = C_1\left[\exp\left(-C_2(\frac{r}{b}-C_3)^2\right)+\exp\left(-C_2(\frac{r}{b}+C_3)^2\right)\right] \quad (12)$$

$$\frac{(\epsilon b)^{1/3}}{u_c} = C_4\left[\exp\left(-C_5(\frac{r}{b}-C_6)^2\right)+\exp\left(-C_5(\frac{r}{b}+C_6)^2\right)\right], \quad (13)$$

to provide their spatial variated functions (Fig. 2). The empirical coefficients

$$\begin{bmatrix} C_1 \\ C_2 \\ C_3 \end{bmatrix} = \begin{bmatrix} 0.2006 \\ 1.4147 \\ 0.6647 \end{bmatrix}, \begin{bmatrix} C_4 \\ C_5 \\ C_6 \end{bmatrix} = \begin{bmatrix} 0.2458 \\ 1.2498 \\ 0.6594 \end{bmatrix}$$

are obtained using least-square best-fitting. The turbulence length and time scales L_E and T_E in Eq. (9) can then be estimated from Eqs. (10) and (11) at any location using σ (or k) and ϵ. Fig. 2 shows that the RMS turbulent fluctuation is about 20 % of the jet centerline velocity and decreases to nearly zero at two Gaussian jet half-width.

With the autocorrelation function, the turbulent fluid fluctuation can be generated by

$$\mathbf{u}'_{f,i+1} = R_i\mathbf{u}'_{f,i} + \boldsymbol{\chi}\sqrt{(1-R_i^2)}\sigma, \quad (14)$$

where $\boldsymbol{\chi}$ is randomly generated numbers (in x, y, z-directions) following a Gaussian distribution with zero mean and unit variance.

3.5 Numerical implementation

Due to the stochastic nature, $N_p = 50000$ particles are used in each jet simulation. This number of particles gives less than 5 % difference in the predicted bottom deposition profile in different numerical realizations of the same experiment. The total duration of each numerical jet experiment is 5 minutes. The particles are released at the end of the zone of established flow ($x = 6.2D$) according to a Gaussian distribution and tracked until they reach the level of the bottom tray (z_b in Fig. 1). Particle tracking calculations have been performed for all experiments in Table 1 using a time-step of 0.001 s, much less than the characteristic time scale of jet turbulence T_E (in the order of 0.05—0.5 s). Computation time for a single simulation is typically 1–2 min on an Intel Xeon 3.3 GHz processor PC. With the Basset force included, the simulation time is 3–4 times of the one without the Basset force term.

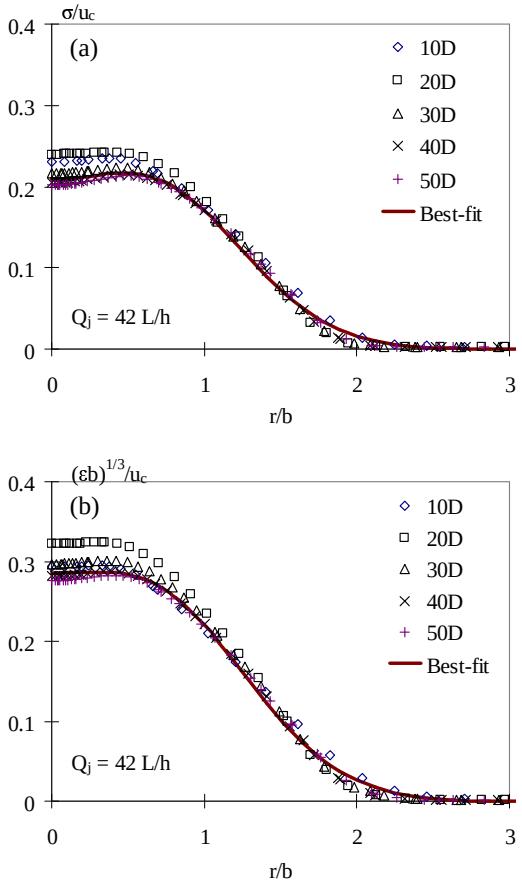

Figure 2. Self-similar turbulent velocity fluctuation and profiles rate dissipation, predicted by CFD model (symbols) and fitted with empirical equations (lines), **(a)** RMS turbulent velocity fluctuation, Eq. (12), **(b)** Turbulent energy dissipation rate, Eq. (13). $D = 6$ mm

4 Experiments

Laboratory experiments of horizontal sediment-laden jets were carried out in a 1m × 1m × 0.45m deep water tank with a horizontal 6mm diameter nozzle located in the middle position of the tank wall and $z_b = 15$cm above the tank bottom (Fig. 1). Steady jet flow was supplied from an overhead tank and measured by a calibrated rotameter. The sediment particles were fed to the jet flow at a constant rate using an hourglass. Sediment bottom deposition profiles were measured using a collection tray and cross-sectional sediment concentrations were measured using particle imaging (Lee et al., 2013). Details of the experiments are described in Chan (2013) (plastic), Lee (2010) (glass) and Li (2006) (sand).

Table 1 summarises the experiments used for comparison with the numerical predictions. A total of 36 experiments were reported, covering a range of initial jet velocity ($u_0 = 0.29-0.88\,\mathrm{m\,s^{-1}}$), particle diameters ($d = 115-716\,\mu\mathrm{m}$) and densities ($\rho_p = 1.16-2.65\,\mathrm{g\,cm^{-3}}$).

Table 1. Summary of horizontal sediment-laden jet experiments for bottom deposition and cross-sectional sediment concentration measurement. Jet diameter $D = 6$ mm, water viscosity $\nu = 10^{-6}$ m^2 s^{-1}.

Particle Type	Particle diameter d (μm)	Settling velocity w_s (cm s^{-1})	Particle Reynolds Number $Re_p = \frac{w_s d}{\nu}$	Jet flow rate Q_j (L h^{-1})	Jet velocity u_0 (m s^{-1})	Jet Reynolds Number $Re = \frac{u_0 D}{\nu}$	Sediment concentration C_0 (g L^{-1})	Momentum/ settling length scale l_m/D
Present study, sediment bottom deposition and concentration measurement								
Plastic (IP3) $\rho_p = 1.14$ g cm^{-3}	716	2.06	14.7	30, 40, 50, 60, 70, 80	0.29–0.79	1740–4740	1.17–3.75	13.3–35.2
Plastic (MF) $\rho_p = 1.5$ g cm^{-3}	347	2.20	7.6	40, 50, 60, 70, 80	0.39–0.79	2340–4740	0.47–0.82	15.8–31.8
Li (2006), sediment bottom deposition measurement, $\rho_p = 2.65$ g cm^{-3}								
Coarse sand	166	1.98	3.3	50, 54, 58, 62, 66	0.49 - 0.65	2940–3900	3.39–4.49	22.2–29.2
Fine sand	133	1.41	1.9	30, 34, 38, 42, 46, 50, 54, 58	0.30–0.57	1800–3420	3.93–7.73	18.5–35.7
Lee (2010), sediment bottom deposition and concentration measurement, $\rho_p = 2.5$ g cm^{-3}								
Glass 215	215	2.64	5.7	60, 70, 80, 90	0.57–0.86	3970–5650	3.39–4.49	18.9–28.3
Glass 180	180	1.83	3.3	50, 60, 70, 80	0.48–0.76	2980-4660	2.32–3.71	20.6–32.9
Glass 115	115	1.03	1.2	40, 50, 60, 70	0.38–0.67	2630-4430	1.03–1.83	32.9–57.6

5 Results and discussion

5.1 Bottom deposition profile

The particle tracking model predicts well the 1-D deposition pattern (transverse (y) direction is lumped) of Lee (2010)'s experiments of spherical glass particles (Fig. 3a–c) and Li (2006)'s experiments using natural sand (Fig. 3d). A close examination of the deposition profiles of G180 particles ($d = 180$ μm, Fig. 3b) and plastic IP3 particles ($d = 716$ μm, Fig. 3e) reveals that the plastic particle deposition profile has a peak located further away ($x_{sm} = 0.18$ m) than that of G180 particles (0.14 m), despite the particles have similar w_s. This reflects the particle inertia effect in reducing the settling velocity in turbulent jet flow. The particle Reynolds number Re_p of plastic particles, which is a measure of the particle inertia, is much larger than that of G180 particles (14.7 vs 3.3, Table 1). Model predictions are also well-compared with the experimental data of plastic particles (Fig. 3e–f).

Sensitivity study has been carried out to investigate the importance of Basset force. By excluding the Basset force from the equation of motion, the predicted 1-D bottom deposition profiles are compared to the one with Basset force. Fig. 3 shows that removing the Basset force does not have a significant impact on the predicted bottom deposition profile. Basset force is the sum of relative velocity changes which diminishes with the square root of time. Due to the fluctuating nature of turbulence, the acceleration of relative velocities tends to cancel out each other during the integration. Thus the overall effect of Basset force in predicting the particle deposition or concentration is not significant. A simple equation of motion consisting of buoyancy, drag, fluid acceleration and added-mass terms is sufficient as these terms pose little computation demand to the numerical solution.

In terms of 2-D deposition profiles (Fig. 4), the predicted deposition patterns (Basset force excluded) compare reasonably well with the observations. The sedimentation pattern is similar to many reported river mouth deposition patterns in jet-like flows, which will eventually leads to the bifurcation of river jet and the formation of delta (Edmonds and Slingerland, 2007). The measured deposition profile is not symmetric in the transverse direction. Cross-section particle concentration measurement (Lee et al., 2013) shows that the particles fall out with an inclined trajectory from the turbulent region of the jet. The particle trajectories tend to swing across the cross-section periodically due to the slowly changing external entrainment flow induced by the large-scale jet eddy structures interacting with the tank bottom (also observed in Rowland et al. (2007) and Mariotti et al. (2013) in a 2-D plane jet flow) and the finite-sized tank. The instabilities result in the increased transverse spread of the observed deposition profiles.

5.2 Cross-section sediment concentration

Sediment concentration measured in the jet cross-section ($y - z$ plane) is compared with the predicted concentration profiles by transforming particle mass to concentration. The particle concentration can be evaluated by the average number of particles inside a control volume $\Delta V = \Delta x \Delta y \Delta z$, defined by $\Delta x = 3$ mm, Δy and Δz = one sixth of the local jet top-hat width (the dashed circle in Fig. 5). The predicted

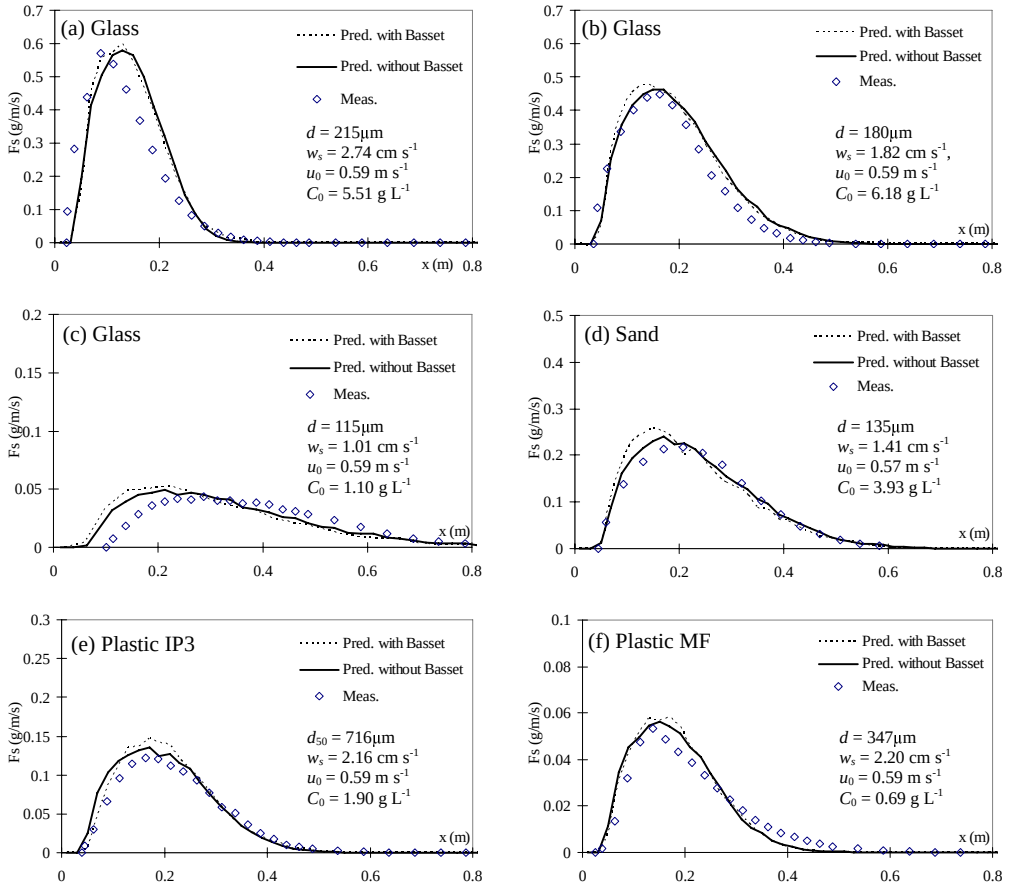

Figure 3. Comparison of predicted and measured 1-D bottom deposition profiles (transversely lumped), with and without the Basset force term.

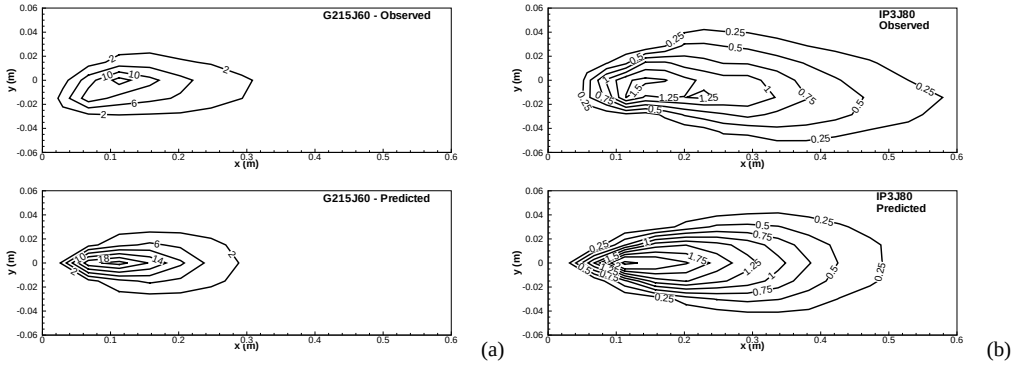

Figure 4. 2-D sediment deposition pattern for **(a)** glass particles 215 μm, $u_0 = 0.59\,\mathrm{m\,s^{-1}}$, $w_\mathrm{s} = 2.65\,\mathrm{cm\,s^{-1}}$, **(b)** plastic IP3 particles 716 μm, $u_0 = 0.79\,\mathrm{m\,s^{-1}}$, $w_\mathrm{s} = 2.02\,\mathrm{cm\,s^{-1}}$. Contours in $\mathrm{g\,m^{-2}\,s^{-1}}$.

cross-sectional concentration profiles for plastic IP3 particles compare very well with the experimental measurements (Fig. 5), showing a typical horseshoe profile. For $x < l_\mathrm{m}$ (Fig. 5a), the maximum concentration is well defined inside the jet top-hat turbulent region. At this location, the centerline $u_\mathrm{c} = 0.3\,\mathrm{m\,s^{-1}}$ and $\sigma = 0.06\,\mathrm{m\,s^{-1}}$ (from Fig. 2), significantly greater than the settling velocity $w_\mathrm{s} = 0.022\,\mathrm{m\,s^{-1}}$. The settling of particles is counter-balanced by jet turbulence and the entrainment flow, despite some sediment starts to settle out at the jet edge with lower turbulence. This region corresponds to the initial rising side of the deposition curve (Fig. 3). For $x > l_\mathrm{m}$ (Fig. 5b), the particle cloud separates significantly from the water jet. At this location, the centerline $u_\mathrm{c} = 0.07\,\mathrm{m\,s^{-1}}$ and $\sigma = 0.015\,\mathrm{m\,s^{-1}}$, lower than the settling

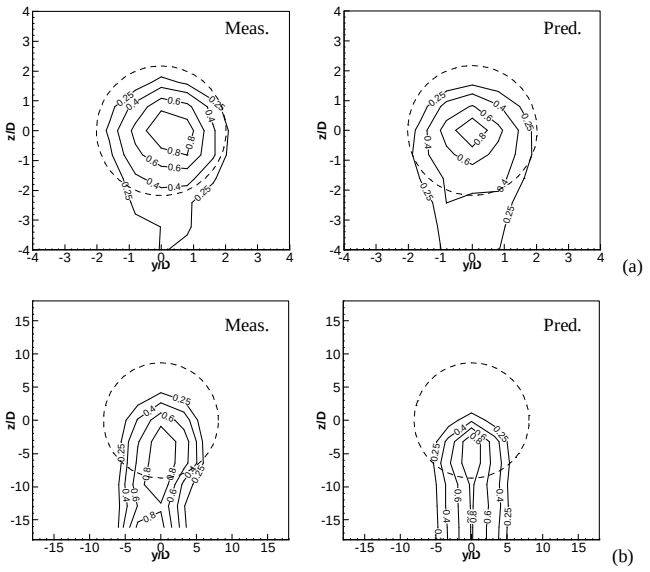

Figure 5. Comparison of predicted and measured profiles of cross-sectional sediment concentration normalized against the maximum concentration at the section $C/C_{\max}$, plastic IP3 particle, $u_0 = 0.59\,\mathrm{m\,s^{-1}}$, $w_s = 2.2\,\mathrm{cm\,s^{-1}}$, $l_m = 34.5D$ **(a)** $x = 12.5D < l_m$, **(b)** $x = 50D > l_m$. $D = 6\,\mathrm{mm}$. The dashed circle is the jet top-hat profile defined by $b_T = \sqrt{2}\beta x$ (Lee and Chu, 2003).

velocity. A complete horseshoe profile appears as all the concentration contours are no longer closed and the line of maximum concentration is located below the top-hat jet region. This corresponds to the gradually falling tail of the deposition curve. These profiles demonstrate that jet turbulence has a very significant effect on the distribution of sediment concentration and deposition pattern by modifying the effective sediment settling velocity. In the measurement (Fig. 5b), the horseshoe trail is often skewed to one side reflecting the complex changing external entrainment flow induced by jet large eddies.

6 Conclusions

A 3-D stochastic particle tracking model is developed to predict the mixing and deposition of horizontal sediment-laden jets in stagnant water. It adopts a autocorrelation function that accounts for the trapping of particles in turbulent eddies and solves the governing equation of particle motion. Analytical mean jet flow solutions are used, with RMS turbulent velocity fluctuations modelled with best-fitted self-similar profiles derived from CFD solution of a pure jet. Model predictions of deposition and concentration profiles of horizontal sediment-laden jets are in excellent agreement with experimental data. A sensitivity study shows that the computationally demanding Basset history force can be neglected for all kind of particles used in present experiments, greatly simplifying the equation of motion and reducing the computation time.

Unlike traditional Eulerian prediction of sediment transport which requires substantial calibration effort to the settling velocity, the present particle model does not require any empirical adjustment/reduction of particle settling velocity to account for the effect of turbulence. The particle tracking method proposed here can be applied to study the deposition and morphological evolution resulted from turbulent jet-like river flows, provided that the flow and turbulence fields, and sediment properties are known.

Acknowledgements. This research is supported by a grant from the Hong Kong Research Grants Council (RGC HKU719408) and in part by a grant from the University Grants Committee of Hong Kong (Project No. AoE/P-04/04) to the Area of Excellence (AoE) in Marine Environment Research and Innovative Technology (MERIT).

References

Bleninger, T., Carmer, C. V., Jirka, G., and Neves, M.: Sedimentation from low concentration particle-laden jets, Proc. 2nd Int. Conf. Marine Waste Water Discharges, Istanbul, Turkey, 16–20 September, 2002.

Chan, S. N.: Mixing and Deposition of Sediment-Laden Buoyant Jets, PhD thesis, The University of Hong Kong, January 2013.

Chan, S. N., Lee, K. W. Y., and Lee, J. H. W.: Numerical modelling of horizontal sediment-laden jets, Environ. Fluid Mech., 14, 173–200, 2014.

Clift, R., Grace, J. R., and Weber, M. E.: Bubbles, Drops and Particles, Dover Publications, 1978.

Cuthbertson, A. J. S. and Davies, P. A.: Deposition from Particle-Laden, Round, Turbulent, Horizontal, Buoyant Jets in Stationary and Coflowing Receiving Fluids, J. Hydraul. Eng.-ASCE, 134, 390–402, 2008.

Edmonds, D. A., and Slingerland, R. L.: Mechanics of river mouth bar formation: Implications for the morphodynamics of delta distributary networks. J. Geophys. Res., 112, F02034, doi:10.1029/2006JF000574, 2007.

Fischer, H. B., List, E. J., Koh, R. C. Y., Imberger, J., and Brooks, N. H.: Mixing in Inland and Coastal Waters, Academic Press, 483 pp., 1979.

Lamb, H.: Hydrodynamics, Cambridge University Press, 738 pp., 1932.

Lane-Serff, G. F. and Moran, T. J.: Sedimentation from buoyant jets, J. Hydraul. Eng.-ASCE, 131, 166–174, 2005

Launder, B. E. and Spalding, D. B.: The numerical computation of turbulent flows. Comput. Method. Appl. M., 3, 269–289, 1974.

Lee, J. H. W. and Chu, V. H.: Turbulent Jets and Plumes: A Lagrangian Approach, Kluwer Academic Publishers, 390 pp., 2003.

Lee, K. W. Y.: Mixing of sediment-laden jet, PhD thesis, The University of Hong Kong, 2010.

Lee, K. W. Y., Li, A. C. Y., and Lee, J. H. W.: Structure of a horizontal sediment-laden momentum jet, J. Hydraul. Eng.-ASCE, ASCE, 139, 124–140, 2013.

Li, A. C. Y.: Theoretical modeling and experimental studies of particle-laden plumes from wastewater discharges, M. Phil. thesis, The University of Hong Kong, 2006.

Mariotti, G., Falcini, F., Geleynse, N., Guala, M., Sun, T., and Fagherazzi, S.: Sediment eddy diffusivity in meandering turbulent jets: Implications for levee formation at river mouths, J. Geophys. Res. Earth Surf., 118, 1908–1920, 2013.

Nielsen, P.: Coastal Bottom Boundary Layers and Sediment Transport, Advanced Series on Ocean Engineering – Vol.4, World Scientific, 1992.

Rowland, J. C., Stacey, M. T., and Dietrich, W. E.: Turbulent characteristics of a shallow wall-bounded plane jet: Experimental implications for river mouth hydrodynamics, J. Fluid Mech., 627, 423–449, 2007.

Shih, T. H., Liou, W. W., Shabbir, A., Yang, Z., and Zhu, J.: A new k-ϵ eddy viscosity model for high Reynolds number turbulent flows, Comput. Fluids, 24, 227–238, 1995.

Wright, L. D.: Sediment transport and deposition at river mouths: A synthesis, Geol. Soc. Am. Bull., 88, 857–868, 1977.